Paper:

Space MMF Harmonic Rotor Losses under Healthy and Open Circuit Conditions

Xing Guan[1], Zhen Chen[*1], Member, IEEE, and Yumeng Li[2]

[1]Beijing Institute of Technology, No. 5, South Street, Zhongguancun, Haidian District, Beijing
Email:guan-xing@163.com, chenzhen76@bit.edu.cn
[2] Beijing Institute of Control Engineering, No. 16, South 3rd. Street, Zhongguancun, Haidian District, Beijing
Email:liyumeng2015@126.com

Abstract. Rotor eddy current losses of a five phase dual-rotor permanent magnet synchronous machine (DR-PMSM) are investigated in both healthy working condition and open circuit fault conditions in this paper. The studied eddy current losses are induced by harmonics of stator magneto-motive force (MMF). The eddy current losses are calculated by finite element method (FEM) using an improved point current model to generate MMFs for different conditions. The calculation results are analyzed and applied in thermal analysis. Finally, experimental measurements and validations are conducted.

Keywords: Eddy-current loss, magneto-motive force, space harmonics, open circuit fault.

1. Introduction

Fractional-Slot concentrated windings permanent magnet synchronous machines (FSCW-PMSM) are applied in various industrial applications thanks to high power density and high efficiency [1-3]. Multi-phase FSCW-PMSM emerged to meet rigid need of high reliability in electric vehicle and aerospace industries. However, FSCW configurations are characterized by substantial stator magneto-motive force (MMF) harmonics which induce eddy currents and generate heat. Overheat can cause demagnetization of Permanent magnets (PMs) and shortened lifetime of the PMSMs [4, 5]. Thus analysis and evaluation of eddy current losses induced by MMF harmonics play a significant role in machine design and operation.

Rotor eddy current losses have been an issue full of interest [6-13]. The rotor eddy current losses are mainly composed of two loss parts, that are P_r and P_s. P_r is caused by relative displacement of the magnets with regard to the slotted structure of the stator [7, 8]. P_s is induced by stator MMF harmonics asynchronous with the rotating rotor [6, 9-12]. Markovic et al. proposed a framework for P_r calculation based on the assumption that eddy currents are resistance limited. De la Barrière et al. proposed an analytical model for P_r calculation, taking both the diffusion phenomenon and the finite length of the magnet along the rotor yoke into account [8]. Atallah et al. proposed a framework for PM eddy current loss induced by sub-harmonics (harmonics with lower order than the fundamental harmonic) and investigated the eddy current loss reduction effect circumferentially segmenting the rotor magnets [9]. Toda et al. investigated the eddy current losses in modular and conventional topologies of PM machines using finite element (FE) and analytical methods. However, the analytical method got larger error compared with the FE method due to neglecting the slot opening effect [10]. Bianchi et al. developed an eddy current model for fast calculation of the eddy current losses induced by each order stator MMF harmonics [6, 12].

For multi-phase fault tolerant machines, there are various working conditions to explore, such as one or two phases open circuit conditions and corresponding fault tolerant working conditions [14, 15]. Under fault operation can be treated as kind of sub-normal working condition. Fault tolerant control methods are applied in order to obtain smooth output torque under open circuit fault working conditions. However, fault tolerant control methods also bring undesired MMF harmonics which induce extra eddy current losses. The interaction between the no-load harmonics and stator MMF harmonics affects rotor eddy current losses [16, 17]. Optimal Torque Control may lead to significant increase in the eddy-current loss in the permanent magnets [18]. Eddy current loss analysis under fault conditions expands the picture of machine rotor eddy current loss research.

2. Point Current Model

When analyzing the influence of stator MMF harmonics on eddy current loss of rotor back iron and magnets, an equivalent current sheet [6], which is applied to replace the stator, as shown in Fig. 1. The model is a fast approach to evaluate eddy current loss of a specific harmonic order. However, the rotor back iron eddy current loss induced by stator MMF is influenced by non-linear material characteristics and sensitive to the BH value of rotor back-iron [19]. Thus the rotor eddy current loss calculated from the point current model with no stator iron contains unneglectable error. On the other hand, the DR-PMSM is of magnetic decoupled design. Direct application of the no-

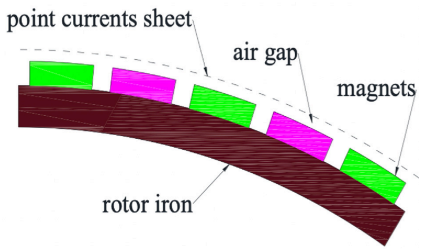

Fig. 1. Point current model without stator iron of PMSM for eddy current calculation.

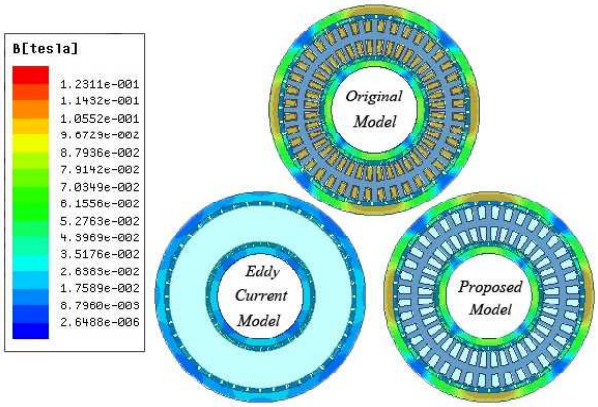

Fig. 2. Stator magnetic flux density magnitude distribution in rotor area.

stator-iron point current model adds mutual coupling effects of inner and outer machine. Based on the mentioned two concerns and the point current model mentioned in [6], the point current model with stator iron is proposed.

The proposed point current model is obtained by replacing the stator windings with two equivalent point current sheets along the stator to air gap boundaries of inner and outer side. As shown in Fig. 2, the magnetic flux density distribution in the magnet and rotor back iron area can be kept as approximate as possible to the original machine model.

When analyzing the impact of stator harmonics on eddy current loss of rotor back iron and magnets. The amplitude $\dot{I}_{nk}$ and initial phase angle α_{nk} of the k-th point current from the initial position of the n-th stator MMF space harmonic is given as [13]:

$$\dot{I}_{nk} = \frac{2\pi n U_{sn}}{N_p} \quad . . . . . (1)$$

$$\alpha_{nk} = n \cdot \theta_k \quad . . . . . (2)$$

where U_{sn} is the amplitude of the stator MMF harmonic, N_p is the number of point currents split along the circumference of the inner or outer stator iron to air gap boundary, and θ_k is the mechanical angle of the k-th point current along the circumference of the stator to air gap boundary of unit motor. The k-th point current for n-th order stator MMF harmonic in the rotor reference frame component along the current sheet is expressed as:

$$I_{nk} = \dot{I}_{nk} sin(2\pi f_n t - \alpha_{nk}) \quad . . . . . (3)$$

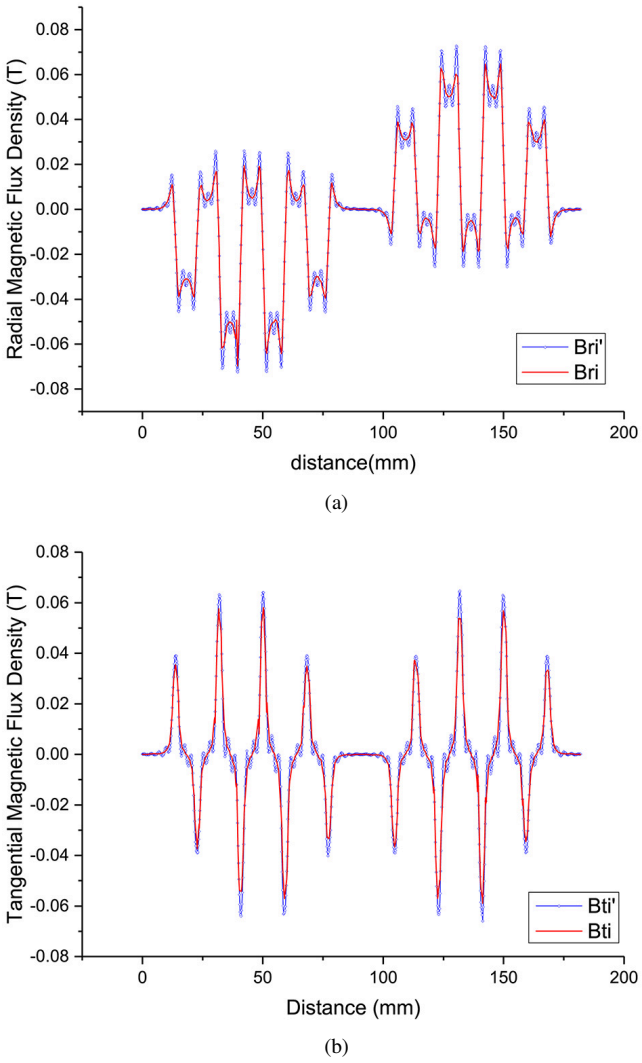

Fig. 3. Magnetic flux density of inner rotor. (a) Radial. (b)Tangential.

Where f_n is the frequency of the n-th stator MMF harmonic.

The point currents of 1st to 60th order are superimposed to get the approximated magnitude distribution of the stator MMF. The supplied k-th point current along the circumference of the stator to air gap boundary of unit motor is expressed as:

$$I_{pk} = \sum_{i=1}^{60} I_{ni} \quad . . . . . (4)$$

The magnetic flux density distribution along the circumferential boundary of inner air-gap of the original model (Bri, Bti) and the proposed model (Bri', Bti') are depicted as Fig. 3. As it can be seen form Fig. 3, the distributions of the original and proposed model are slightly different on the magnet edges, which is caused by the Gibbs phenomenon. Except that, as shown in Fig. 3, the magnetic flux density distribution of the proposed model match well with that of the original model.

Table 1. Rotor Losses under Different Conditions.

Conditions	Loss(W)	Conditions	Loss(W)
Case 0	8.4	–	–
Case 1.1	6.28	Case 1.1TC	11.26
Case 2.1	4	Case 2.1TC	26.8
Case 2.4	4.02	Case 2.4TC	14.57

3. Eddy Current Losses Analysis

This paper mainly focuses on the rotor eddy current losses induced by stator MMF harmonics. In order to evaluate the eddy current loss performance of the DR-PMSM in a wide and clear view, the following rotor loss analysis is conducted in aspect of total rotor loss and harmonic loss spectrum respectively.

The calculated losses are components of P_s in [6] for fast eddy current estimation. The effectiveness of the investigation of the harmonic losses are investigated via time stepped finite element analysis of the point current model. The total eddy current losses induced by asynchronous stator MMF space harmonics are obtained, the results are shown in Table 1. As shown Table 1, the fault tolerant operation brings more losses. Thus the following harmonic loss analysis is focused on the eddy current losses under healthy and fault tolerant operations.

In harmonic losses spectrum aspect, based on the proposed point current model, the eddy current loss over harmonic order n are obtained using finite element calculation. The eddy current losses induced by harmonics higher than 11th harmonic are negligible compared with the losses induced by 1st to 9th harmonics. Hence, the following analysis mainly focus on the eddy current losses induce by 1st, 3rd, 7th and 9th stator MMF harmonics.

3.1. Case 0

For the healthy working condition, the eddy current losses induced by stator MMF harmonics in the rotor back iron and magnets are depicted as Fig. 4. In Fig. 4 and the following relevant Figures, "im", "ir", "om" and "or" is short for inner magnets, inner rotor back iron, outer magnets and outer rotor back iron, respectively.

It is evident in Fig. 4 that the maximum eddy current losses are induced by the 1st harmonic component $cos(\omega t - \psi)$, and the eddy current losses in the rotor back iron are much higher than that in the magnets. Although, the inner and outer motor have the same number of slots and magnet poles, larger dimensions lead to more losses induced in outer motor.

3.2. Case 1.1TC

For one phase open circuit working condition with tolerant control, the eddy current loss induced by stator MMF harmonics in the rotor back iron and magnets are depicted as Fig 5.

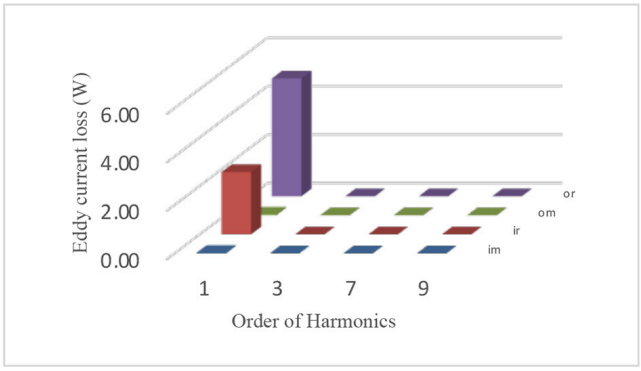

(a)

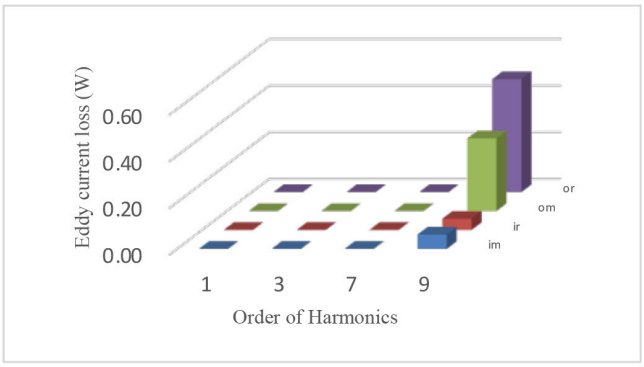

(b)

Fig. 4. Eddy current losses over harmonic order in case 0. (a) $cos(\omega t - n\psi)$. (b)$cos(\omega t + n\psi)$.

After tolerant control, the eddy current losses induced by harmonic component $cos(\omega t - \psi)$ are kept nearly equal to that of healthy working condition while the eddy current losses induced by harmonic component $cos(\omega t + \psi)$ becomes higher. Compared to healthy working condition, the main eddy current loss increment of fault tolerant control mainly comes from 3rd harmonic component $cos(\omega t + 3\psi)$.

3.3. Case 2.1TC

For the two adjacent phases open circuit with tolerant control working condition, the eddy current losses induced by stator MMF harmonics in the rotor back iron and magnets are depicted as Fig 6.

It's clear that when two adjacent phases get open circuited, the applied tolerant control brings much more eddy current losses mainly induced by harmonic component $sin(\omega t + 3\psi)$ in outer rotor back iron.

3.4. Case 2.4TC

For the two non-adjacent phases open circuit condition, the eddy current losses induced by stator MMF harmonics in the rotor back iron and magnets are depicted as Fig 7.

From Fig 7, the main eddy current losses increment brought by fault tolerant control are induced by harmonic components of $sin(\omega t + 3\psi)$ in rotor back iron parts.

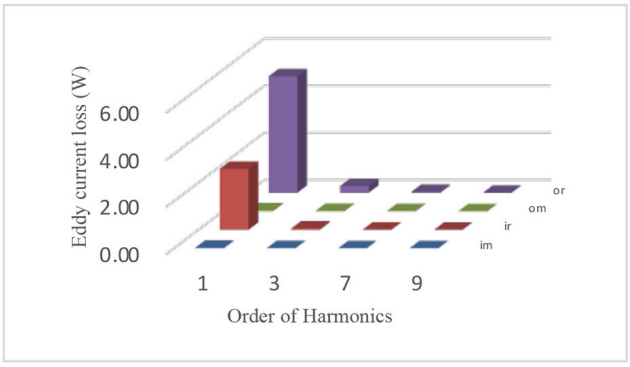

(a)

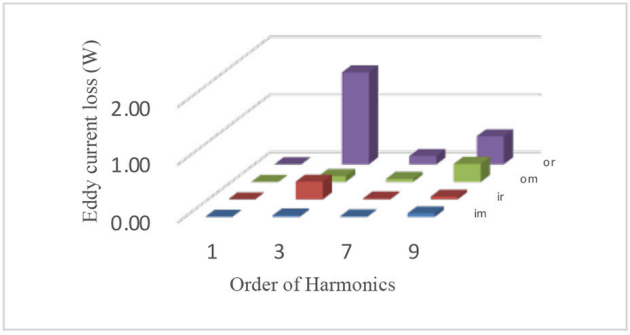

(b)

Fig. 5. Eddy current losses over harmonic order in case 1.1TC. (a) $cos(\omega t - n\psi)$. (b)$cos(\omega t + n\psi)$.

Table 2. Thermal Parameters of Machine Materials.

	Density kg/m^3	Thermal conductivity W/(m·K)	Specific heat capacity J/(kg·K)
Winding copper	8900	387	407
Slot insulation	2300	0.16	1250
PM	7400	8.923	502.3
Stator core	7700	55.6	504
rotor iron	7870	51.9	448

4. Thermal Analysis

The parameters for the inner and outer air gap and motor materials are listed in Table 2. This paper mainly focus on the temperature distribution of the machine under rated working condition (working at 600 rpm with load 16.56 N·m) to evaluate the losses and the machine performance.

The 3D model of the DR-PMSM is shown in Fig. 8. The temperature distribution of the DR-PMSM under rated working condition is depicted in Fig. 9. The highest temperature is 37.63°C which is much lower than the maximum working temperature (180°C) of H class insulation material. The maximum temperature of the magnet region is 31.8°C which is also much lower than maximum

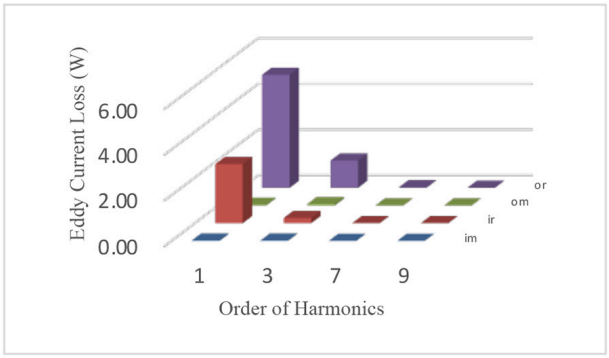

(a)

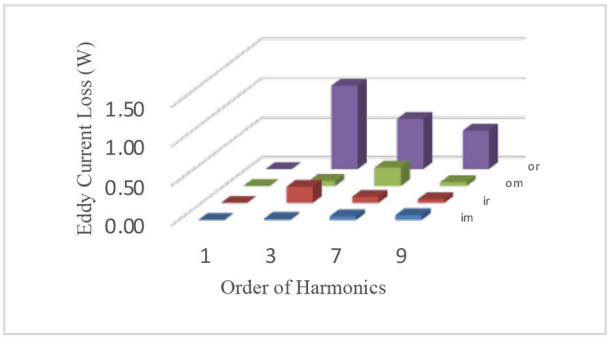

(b)

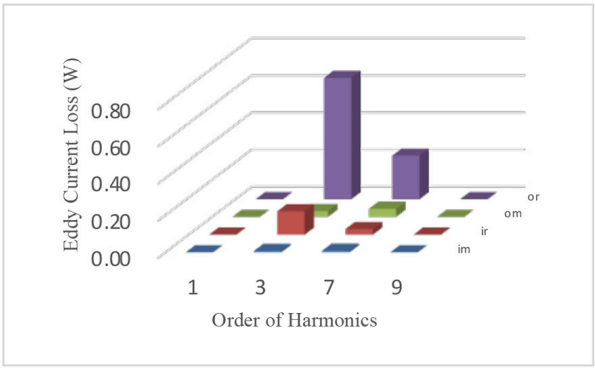

(c)

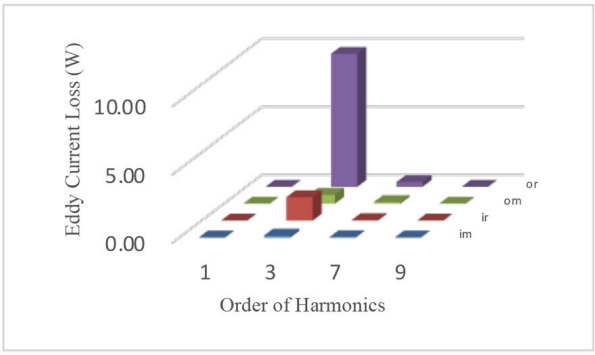

(d)

Fig. 6. Eddy current losses over harmonic order in case 2.1TC. (a) $cos(\omega t - n\psi)$. (b)$cos(\omega t + n\psi)$. (c) $sin(\omega t - n\psi)$. (d)$sin(\omega t + n\psi)$.

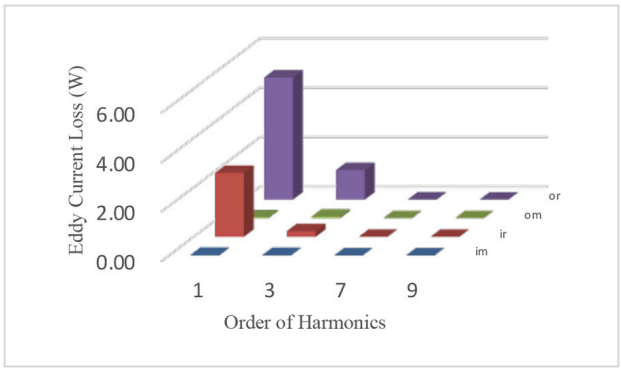

(a)

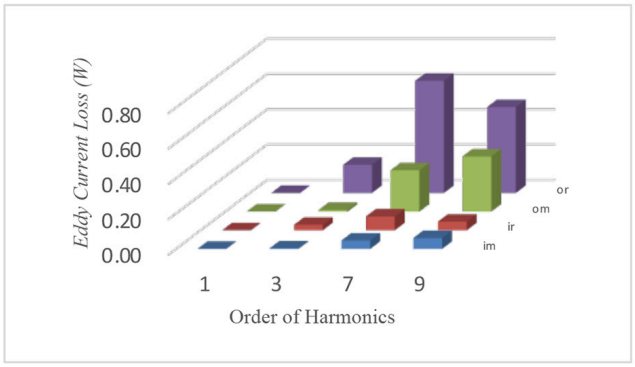

(b)

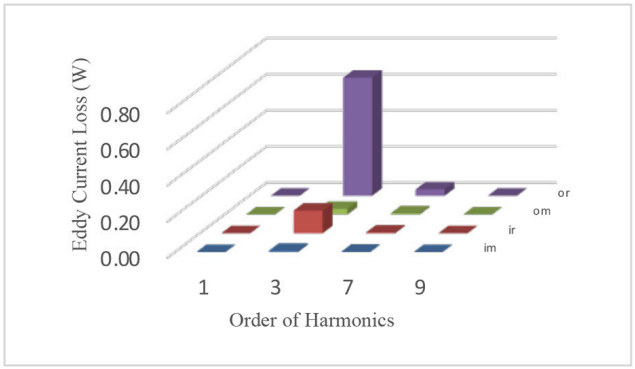

(c)

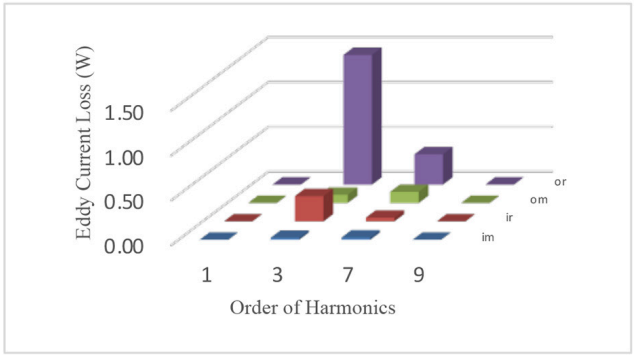

(d)

Fig. 7. Eddy current losses over harmonic order in case 2.4TC. (a) $cos(\omega t - n\psi)$. (b)$cos(\omega t + n\psi)$. (c) $sin(\omega t - n\psi)$. (d)$sin(\omega t + n\psi)$.

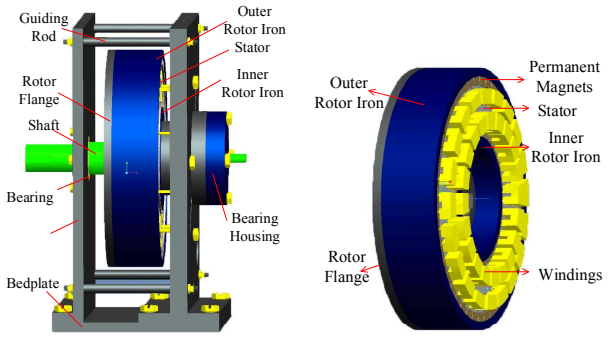

(a) (b)

Fig. 8. 3D model of the DR-PMSM. (b)Assembly. (b)Stator and rotor.

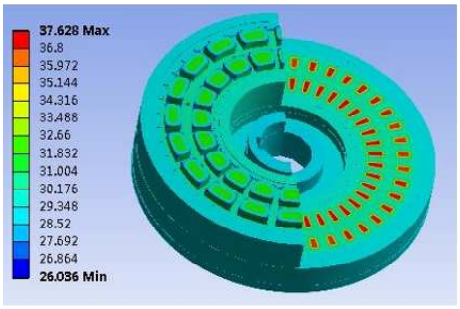

Fig. 9. Temperature field distribution of the DR-PMSM under rated working condition.

working temperature (150°C) of the magnets.

5. Experiments

A prototype of the five-phase fault-tolerant DR-PMSM is manufactured to validate the analysis results, as shown in Fig. 10. The average value of the neighbor windings is used as the measured temperature. In the experiment, the DR-PMSM is operated with the load of 2.1N·m at the speed of 92rpm and the temperature of the ambient air is 24°C.

The measured and simulated temperature rise of inner and outer motor are depicted in Fig. 11. Comparing the simulated and measured results, the maximum error of steady state temperature is about 0.3°C. The reasons may be the calculated error of different parts of the transfer coefficient or the error measuring instrument. However, the temperature rise trends are consistent in general, and it validates the simulated method and calculated results.

6. Conclusion

In this paper, the stator MMF space harmonics and the eddy current losses induced under healthy and open circuit with tolerant control conditions are investigated.

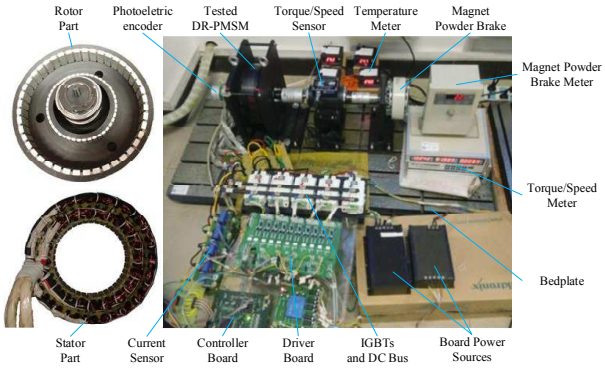

Fig. 10. The components and test platform of the prototype machine.

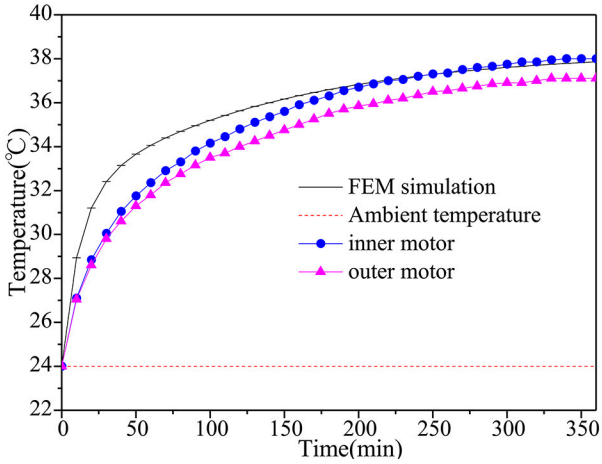

Fig. 11. The measured and simulated temperature rise.

The stator MMF harmonic components under healthy and fault tolerant conditions are analyzed. The eddy current model is verified by the original model. The temperature rise experiments are conducted to verify the original model and the thermal reliability of the DR-PMSM. The following conclusions can be obtained:

1) The proposed point current model can obtain accurate eddy current losses and be used in harmonic eddy current loss analysis. The main eddy current losses are induced by odd harmonics.

2) Stator space harmonic components $cos(\omega t - \psi)$ and $cos(\omega t + 9\psi)$ exists in healthy and all the open circuit fault conditions, The amplitudes of the two series harmonics are nearly the same under healthy and fault tolerant condition.

3) Fault tolerant control techniques used in [11] can bring more eddy current losses because the injected currents bring 3rd stator MMF space harmonics.

References:

[1] A. M. E.-. Refaie, "Fractional-Slot Concentrated-Windings Synchronous Permanent Magnet Machines: Opportunities and Challenges," IEEE Transactions on Industrial Electronics, vol. 57, no. 1, pp. 107-121, 2010.

[2] K. Huilin, Z. Libing, and W. Jin, "Harmonic winding factors and MMF analysis for five-phase fractional-slot concentrated winding PMSM." pp. 1236-1241.

[3] D. Ishak, Z. Q. Zhu, and D. Howe, "Eddy-current loss in the rotor magnets of permanent-magnet brushless machines having a fractional number of slots per pole," Magnetics, IEEE Transactions on, vol. 41, no. 9, pp. 2462-2469, 2005.

[4] C. Ruschetti, C. Verucchi, G. Bossio et al., "Rotor demagnetization effects on permanent magnet synchronous machines," Energy Conversion and Management, vol. 74, pp. 1-8, 10//, 2013.

[5] H. Torkaman, R. Moradi, A. Hajihosseinlu et al., "A comprehensive power loss evaluation for Switched Reluctance Motor in presence of rotor asymmetry rotation: Theory, numerical analysis and experiments," Energy Conversion and Management, vol. 77, pp. 773-783, 1//, 2014.

[6] N. Bianchi, S. Bolognani, and E. Fornasiero, "An Overview of Rotor Losses Determination in Three-Phase Fractional-Slot PM Machines," Industry Applications, IEEE Transactions on, vol. 46, no. 6, pp. 2338-2345, 2010.

[7] M. Markovic, and Y. Perriard, "A simplified determination of the permanent magnet (PM) eddy current losses due to slotting in a PM rotating motor." pp. 309-313.

[8] O. Barriere, S. Hlioui, H. Ben Ahmed, et al. "An Analytical Model for the Computation of No-Load Eddy-Current Losses in the Rotor of a Permanent Magnet Synchronous Machine"[J]. IEEE Transactions on Magnetics, vol.52, no.6, pp. 1-13, 2016.

[9] K. Atallah, D. Howe, P. H. Mellor et al., "Rotor loss in permanent-magnet brushless AC machines," IEEE Transactions on Industry Applications, vol. 36, no. 6, pp. 1612-1618, 2000.

[10] H. Toda, X. Zhenping, W. Jiabin et al., "Rotor eddy-current loss in permanent magnet brushless machines," IEEE Transactions on Magnetics, vol. 40, no. 4, pp. 2104-2106, 2004.

[11] Y. Huang, J. Dong, L. Jin et al., "Eddy-Current Loss Prediction in the Rotor Magnets of a Permanent Magnet Synchronous Generator With Modular Winding Feeding a Rectifier Load," IEEE Transactions on Magnetics, vol. 47, no. 10, pp. 4203-4206, 2011.

[12] N. Bianchi, and E. Fornasiero, "Index of rotor losses in three-phase fractional-slot permanent magnet machines," IET Electric Power Applications, vol. 3, no. 5, pp. 381-388, 2009.

[13] N. Bianchi, S. Bolognani, and E. Fornasiero, "An Overview of Rotor Losses Determination in Three-Phase Fractional-Slot PM Machines," IEEE Transactions on Industry Applications, vol. 46, no. 6, pp. 2338-2345, 2010.

[14] Y. M. Li, J. Zhao, Z. Chen et al., "Investigation of a Five-Phase Dual-Rotor Permanent Magnet Synchronous Motor Used for Electric Vehicles," Energies, vol. 7, no. 6, pp. 3955-3984, Jun, 2014.

[15] J. Zhao, X. Gao, B. Li et al., "Open-Phase Fault Tolerance Techniques of Five-Phase Dual-Rotor Permanent Magnet Synchronous Motor," Energies, vol. 8, no. 11, pp. 12342, 2015.

[16] S. A. Sharkh, N. T. Irenji, and M. Harris, "Effect of power factor on rotor loss in high-speed PM alternators." pp. 346-350.

[17] J. D. Ede, K. Atallah, and G. W. Jewell, "Effects of load conditions on rotor eddy current loss in modular permanent magnet machines." pp. 1328-1333.

[18] J. D. Ede, K. Atallah, W. Jiabin et al., "Effect of optimal torque control on rotor loss of fault-tolerant permanent-magnet brushless machines," IEEE Transactions on Magnetics, vol. 38, no. 5, pp. 3291-3293, 2002.

[19] G. Ugalde, Z. Q. Zhu, J. Poza et al., "Analysis of rotor eddy current loss in fractional slot permanent magnet machine with solid rotor back-iron." pp. 1-6.

[20] J. Bai, Y. Liu, Y. Sui, C. Tong, Q. Zhao, and J. Zhang, "Investigation of the cooling and thermal-measuring system of a compound-structure permanent-magnet synchronous machine," Energies, vol. 7, pp. 1393–1426, 03 2014.